Available online at www.sciencedirect.com
ScienceDirect
Ceramics International 36 (2010) 979–988
CERAMICS INTERNATIONAL
www.elsevier.com/locate/ceramint

Optimization of the sputtering process parameters of GZO films using the Grey–Taguchi method

Chien-Chih Chen [a], Chung-Chen Tsao [b], You -Chiuan Lin [a], Chun-Yao Hsu [a,*]

[a] Department of Mechanical Engineering, Lunghwa University of Science and Technology, No. 300, Sec. 1, Wanshou Rd., Guishan Shiang, Taoyuan 33306, Taiwan, ROC

[b] Department of Automation Engineering, Tahua Institute of Technology, No. 1, Tahua Rd., Chunglin, Hsinchu 30740, Taiwan, ROC

Received 2 May 2009; received in revised form 27 September 2009; accepted 2 November 2009
Available online 29 November 2009

Abstract

This paper examines the optimization of the process parameters of GZO films deposited on polyethylene terephthalate substrates by R.F. magnetron sputtering using the Taguchi method, aiming to obtain highly transparent and conductive films. The influences of the various sputtering factors (R.F. power, sputtering pressure, deposition time, substrate temperature and post-annealing temperature) on electrical resistivity and structural, morphological and optical transmittance of GZO films are analyzed. The electrical resistivity and the optical transmittance of GZO films were improved by post-annealing the substrate during the deposition process. Experimental results indicate the optimal process parameters in GZO films deposited on polyethylene terephthalate substrates can be determined effectively. The electrical resistivity of GZO films is decreased from $1.194 \times 10^{-3}\ \Omega$ cm to $8.627 \times 10^{-4}\ \Omega$ cm and the optical transmittance is increased from 86.148% to 90%, leading to multiple performance characteristics in deposition qualities through the Grey–Taguchi method.

Keywords: Gallium-doped zinc oxide; Transparent conductive oxide; Polymeric substrates; Grey relational analysis; Post-annealing

1. Introduction

Zinc oxide (ZnO), indium tin oxide (ITO) and fluorine-doped SnO_2 transparent conducting films (TCO) have very interesting optical and electrical properties. These materials have been widely investigated for use in light-emitting diodes (LED), liquid crystal displays (LCD), touch panels, amorphous silicon solar cells, transparent heating elements, anti-static films and other optoelectronic devices [1–4]. In addition, zinc oxide (ZnO) films have been the focus of much attention as transparent conductive films because of low cost advantages compared to ITO films, resource availability, non-toxicity, wide energy band gap (~3.3 eV) and high thermal or chemical stability [5]. For ZnO films doped with Ga, the commonly use fabrication techniques include sputtering [6], chemical vapor deposition [7] and sol–gel [8]. Banerjee et al. [9] studied the structural, optical and electrical properties of ZnO thin films (260–490 nm thick) deposited by the direct-current sputtering technique, at a relatively low-substrate temperature (363 K), onto polyethylene terephthalate and glass substrates. Moreover, the effect of doping of Si [10], Al [11] and Ti [12] in ZnO films has also been explored. Highly conductive and transparent gallium-doped zinc oxide (GZO) thin films have been coated at high growth rates by radio frequency (R.F. 13.56 MHz) magnetron sputtering [13]. The films processed at room temperature on soda lime glass substrates using a ceramic oxide target ZnO/Ga_2O_3, a low resistivity of $2.6 \times 10^{-4}\ \Omega$ cm was obtained.

Yu et al. [14] prepared transparent conducting GZO on a glass substrate by the R.F. magnetron sputtering technique at a low-substrates temperature. They studied the effects of post-annealing treatment on the structural, electrical and optical properties. The results point out the average values of optical transmittance can be increased by 2.9% and the electrical resistivity can be decreased by 52.2% compared with unannealing treatment. Fortunato et al. [15] investigated the thickness dependence (from 70 nm to 890 nm) on the electrical, structural, morphological and optical properties of GZO coated on polyethylene naphthalate (PEN) substrates by R.F. magnetron sputtering at room temperature. They found that electrical resistivity is a function of the GZO film thickness. With

* Corresponding author. Fax: +886 2 82094845.
E-mail address: cyhsu@mail.lhu.edu.tw (C.-Y. Hsu).

0272-8842/$36.00
doi:10.1016/j.ceramint.2009.11.019

increasing thickness, up to a value of approximately 300 nm, the resistivity decreases to a minimum value of $6 \times 10^{-4}\ \Omega$ cm. Ma et al. [16] showed that higher temperature helps to promote Ga substitution more easily. Moreover, the morphology of the film is strongly related to the substrate temperature. Gonçalves et al. [17] found the sheet resistance of GZO film increased tremendously almost 6 orders of magnitude between as-deposited and annealed (500 °C). Besides, the variation of optical transmittance of the GZO film was clearly noticeable.

Taguchi method is a powerful approach for increasing experimental efficiency [18–20]. An L_{18} mixed orthogonal table in the Taguchi quality design derives important coating factors. To optimize the process based on the experimental data, the traditional statistical regression requires a large amount of data, leading to difficulty in treating the typical normal distribution of data and the lack of variant factors. In 1982, Grey analysis was first proposed by Dr. Deng to fulfill the crucial mathematical criteria for dealing with poor, incomplete, and uncertain systems [21]. Grey analysis can effectively recommend a method of optimizing the complicated inter-relationships among multiple performance characteristics. In Grey system theory, the Grey relational analysis is a measurement method to analyze the relationship between sequences using less data and multi-factor, which is considered more helpful to the statistical regression analysis.

Plastic materials are substituted for glass substrates in various applications because they are inexpensive, impact resistant, flexible and lighter in weight. The present study describes the electrical and optical properties of transparent conducting ZnO:Ga = 97:3 wt% depositions on cheap polyethylene terephthalate (PET) substrates with the R.F. magnetron sputtering technique. The work examines the effects of deposition parameters (R.F. power, sputtering pressure, deposition time, substrate temperature and post-annealing temperature) on the properties of the GZO films.

2. Taguchi method

2.1. Analysis of the S/N ratio

Taguchi method was used for executing the experiment, employing a generic signal-to-noise (S/N) ratio to quantify present variation. Depending on the particular type of characteristics involved, different S/N ratios may be applicable, including ''lower is better'' (LB), ''nominal is best'' (NB), and ''higher is better'' (HB). The S/N ratios were calculated using the following equations [18–20]:

$$\eta = 10\log(\text{S/N ratio}) \tag{1}$$

$$\text{HB}: \quad (\text{S/N ratio}) = \frac{1}{\sigma^2}, \quad \sigma^2 = \frac{1}{n}\left(\frac{1}{y_1^2} + \frac{1}{y_2^2} + \cdots\cdots + \frac{1}{y_n^2}\right) \tag{2}$$

$$\text{LB}: \quad (\text{S/N ratio}) = \frac{1}{\sigma^2}, \quad \sigma^2 = \frac{1}{n}(y_1^2 + y_2^2 + \cdots\cdots + y_n^2) \tag{3}$$

where η denotes the observed value, that is, the calculated value of the S/N ratio (unit: dB), y_n represents the measure experimental value and n is the repeated number.

2.2. Analysis of variance (ANOVA)

ANOVA and the F-test are used to analyze the experimental data as follows [20]:

$$S_m = \frac{(\sum \eta_i)^2}{18}, \quad S_T = \sum {\eta_i}^2 - S_m \tag{4}$$

$$S_A = \frac{(\sum {\eta_{Ai}}^2)^2}{N} - S_m, \quad S_E = S_T - \sum S_A \tag{5}$$

$$V_A = \frac{S_A}{f_A}, \quad F_{Ao} = \frac{V_A}{V_E} \tag{6}$$

where S_T is the sum of squares due to the total variation, S_m is the sum of squares due to the means, S_A is the sum of squares due to parameter A (A = R.F. power, sputtering pressure, deposition time, substrate temperature and post-annealing temperature). S_E is the sum of squares due to error, η_i is the η value of each experiment (i = 1–18), η_{Ai} is the sum of the i level of parameter A (i = 1, 2 or i = 1, 2, 3), N is the repeating number of each level of parameter A, f_A is the degree of freedom of parameter A, V_A is the variance of parameter A, F_{Ao} is the F-test value of parameter A.

3. Grey relational analysis

The Grey relational analysis can be used to effectively solve complicated inter-relationships among multiple performance characteristics [22–24]. The Grey relational coefficient is [21]:

$$r(x_0(k), x_i(k)) = \frac{\min_i \ \min_k |x_0(k) - x_i(k)| + \zeta \max_i \ \max_k |x_0(k) - x_i(k)|}{|x_0(k) - x_i(k)| + \zeta \max_i \ \max_k |x_0(k) - x_i(k)|} \tag{7}$$

where $x_i(k)$ is the normalized value of the kth performance characteristic in the ith experiment and ζ is the distinguishing coefficient, $\zeta \in [0, 1]$. The value of ζ can be adjusted according to the actual system requirement. The coating parameters are equally weighted in this paper, and therefore ζ is 0.5.

The Grey relational grade is a weighting-sum of the Grey relational coefficient. It is defined as follows [21]:

$$r(x_0, x_i) = \frac{1}{n}\sum_{k=1}^{n} r(r_0(k), x_i(k)) \tag{8}$$

where n is the number of performance characteristics. The Grey relational grade shows the correlation between the reference sequence and the comparability sequence to be compared to. The evaluated Grey relational grade fluctuates from 0 to 1 and equals 1 if these two sequences are identically coincident.

Table 1
Setting of factors and levels in deposition conditions.

Substrate	PET (HSL188)
Target	ZnO:Ga = 97:3 wt%; 99.999% purity; 5.08 cm in diameter
Gas	Argon (99.995%)
Base pressure	0.67×10^{-3} Pa
Substrate-to-target distance	10 cm
Substrate rotate vertical axis	20 rpm

Symbol	Control factor	Level 1	Level 2	Level 3
A	R.F. power (W)	50	100	200
B	Sputtering pressure (Pa)	0.13	0.67	1.33
C	Deposition time (min)	30	60	90
D	Substrate temperature (°C)	Room temperature	50	100
E	Post-annealing temperature (°C)	None	100	200

Table 2
Experimental results for deposition rate and S/N ratio.

Experimental no.	Control factors					Deposition rate (nm/min)		Mean value	Standard deviation	η (dB)
	A	*B*	*C*	*D*	*E*	1	2			
1	1	1	1	1	1	4.482	4.696	4.589	0.151	13.227
2	1	2	2	2	2	5.636	5.587	5.612	0.035	14.981
3	1	3	3	3	3	4.968	4.854	4.911	0.081	13.822
4	2	1	1	2	2	9.562	9.334	9.448	0.161	19.505
5	2	2	2	3	3	11.116	11.283	11.199	0.118	20.983
6	2	3	3	1	1	9.988	10.026	10.007	0.027	20.006
7	3	1	2	1	3	19.916	20.207	20.061	0.205	26.046
8	3	2	3	2	1	21.597	21.625	21.611	0.019	26.693
9	3	3	1	3	2	20.881	20.934	20.907	0.037	26.406
10	1	1	3	3	2	4.751	4.631	4.691	0.085	13.423
11	1	2	1	1	3	4.998	4.925	4.962	0.052	13.911
12	1	3	2	2	1	4.925	4.825	4.875	0.071	13.758
13	2	1	2	3	1	9.686	9.675	9.680	0.008	19.718
14	2	2	3	1	2	11.136	11.573	11.354	0.309	21.098
15	2	3	1	2	3	10.753	10.776	10.764	0.016	20.639
16	3	1	3	2	3	19.464	19.421	19.442	0.030	25.775
17	3	2	1	3	1	22.061	22.036	22.048	0.017	26.867
18	3	3	2	1	2	20.476	20.503	20.489	0.019	26.230

4. Experimental details

The GZO films with different deposition parameters were coated on PET (polyethylene terephthalate) substrates by an R.F. magnetron sputtering system. Before coating, the substrates were ultrasonically cleaned in acetone, rinsed in deionized water and dried in nitrogen. This deposition experiment selects five influential deposition parameters: that is, R.F. power, sputtering pressure, deposition time, substrate temperature and post-annealing temperature. Table 1 shows the factors and levels settings in deposition conditions.

Table 3
ANOVA results for deposition rate.

Factors	Level (dB)			DF	SS	*V*	*F*	$F_{0.05}$	*P* (%)
	1	2	3						
A	13.857	20.327	26.337	2	467.456	233.728	2317.789	4.46	98.95
B	19.618	20.757	20.144	2	3.899	1.950	19.334	4.46	0.83
C	20.095	20.287	20.138	2	0.122	0.061	0.603	4.46	0.03
D	20.090	20.226	20.204	2	0.065	0.032	0.320	4.46	0.01
E	20.047	20.276	20.197	2	0.163	0.081	0.806	4.46	0.03
Error				7	0.706	0.101			0.15
PE				(13)	(1.056)	(0.081)			(0.22)
Total				17	472.411				100

DF: degree of freedom, SS: sum of squares, *V*: variance, *F*: *F*-test, $F_{0.05}$: 95% confidence band, *P*: percentage of contribution, PE: pooled error.

Film thickness was measured using a surface profilometer (α-step; AMBIOS XP-1). Surface morphology was analyzed using a JEOL JSM-6500F field emission scanning electron microscope (FESEM). The structural of the films were determined by X-ray diffraction (Rigaku-2000 X-ray Generator) using Cu Kα radiation with an angle of incidence of 1°. Electrical resistivity was detected by the four-point probe method (Mitsubishi Chemical MCP-T600). The optical transmittance measurement was performed with a UV-VIS spectrophotometer in the wavelength range from 300 nm to 800 nm.

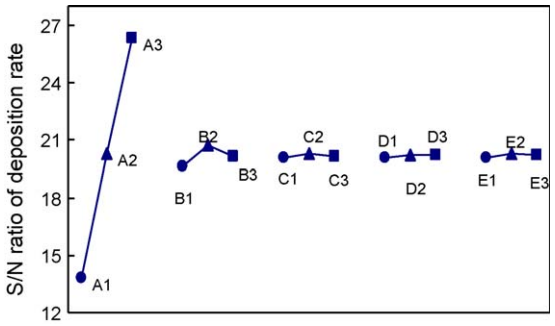

Fig. 1. S/N graph for deposition rate.

5. Results and discussion

Table 2 shows the experimental results of the deposition rate and the corresponding signal-to-noise (S/N) ratios using Eqs. (1) and (3). The ANOVA results for the deposition rate were listed in Table 3. In Table 3, the R.F. power ($P = 98.95\%$) and sputtering pressure ($P = 0.83\%$) had a higher effect on the deposition rate and the best combination to get higher deposition rate is $A_3B_2C_2D_2E_2$. Fig. 1 shows the S/N response graph for deposition rate, indicating an increase in R.F. power to obtain a high deposition rate. Sputtering pressure had little effect on the deposition rate.

Table 4 shows the experimental results for electrical resistivity and the corresponding S/N ratios. Table 5 lists the ANOVA results for electrical resistivity. From Table 5, R.F. power ($P = 93.34\%$) is a significant factor in the deposition process. However, substrate temperature and post-annealing

Table 4
Experimental results for electrical resistivity and S/N ratio.

Experimental no.	Control factors					Resistivity (10^{-3} Ω cm)		Mean value	Standard deviation	η (dB)
	A	*B*	*C*	*D*	*E*	1	2			
1	1	1	1	1	1	14.900	15.300	15.100	0.283	−23.580
2	1	2	2	2	2	9.820	9.731	9.775	0.063	−19.802
3	1	3	3	3	3	7.941	7.790	7.865	0.106	−17.914
4	2	1	1	2	2	5.430	5.571	5.501	0.099	−14.808
5	2	2	2	3	3	4.622	4.341	4.481	0.198	−13.029
6	2	3	3	1	1	6.520	6.641	6.581	0.085	−16.365
7	3	1	2	1	3	1.551	1.670	1.611	0.085	−4.143
8	3	2	3	2	1	1.891	1.962	1.925	0.049	−5.690
9	3	3	1	3	2	1.760	1.640	1.700	0.085	−4.614
10	1	1	3	3	2	7.332	7.011	7.171	0.226	−17.113
11	1	2	1	1	3	6.911	7.080	6.995	0.120	−16.896
12	1	3	2	2	1	7.821	7.651	7.735	0.120	−17.769
13	2	1	2	3	1	6.091	5.920	6.005	0.120	−15.571
14	2	2	3	1	2	5.952	5.793	5.872	0.113	−15.373
15	2	3	1	2	3	5.482	5.661	5.571	0.127	−14.918
16	3	1	3	2	3	1.041	1.110	1.075	0.049	−0.633
17	3	2	1	3	1	1.161	1.270	1.215	0.077	−1.700
18	3	3	2	1	2	1.412	1.340	1.376	0.049	−2.769

Table 5
ANOVA results for electrical resistivity.

Factors	Level (dB)			DF	SS	*V*	*F*	$F_{0.05}$	*P* (%)
	1	2	3						
A	−18.847	−15.013	−3.262	2	791.323	395.662	84.660	4.46	93.34
B	−12.643	−12.085	−12.394	2	0.937	0.468	0.100	4.46	0.11
C	−12.754	−12.183	−12.184	2	1.302	0.651	0.139	4.46	0.15
D	−13.19	−12.273	−11.659	2	7.128	3.564	0.763	4.46	0.84
E	−13.448	−12.415	−11.258	2	14.409	7.204	1.542	4.46	1.70
Error				7	32.715	4.674			3.86
PE				(15)	(56.491)	(3.766)			(6.66)
Total				17	847.814				100

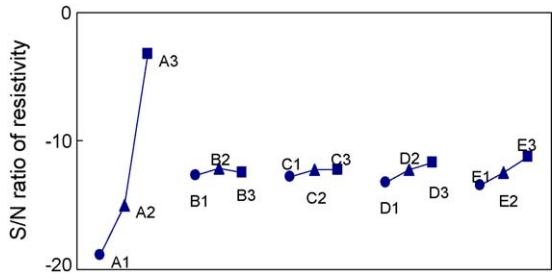

Fig. 2. S/N graph for electrical resistivity.

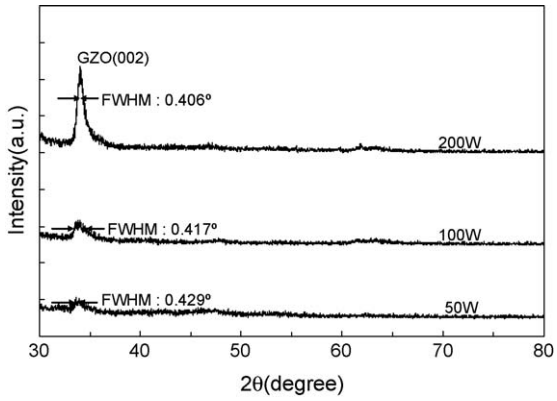

Fig. 3. X-ray diffraction patterns of as-deposited GZO thin films at R.F. power tested after deposition for 60 min at substrate held at room temperature at sputtering pressure of 0.67 Pa.

temperature are useful to reduce the crystallinity of GZO thin film. The best combination is $A_3B_2C_2D_3E_3$ on lower electrical resistivity. Fig. 2 shows the S/N response graph for electrical resistivity. Experimental results point out higher R.F. power, substrate temperature and post-annealing temperature result in lower electrical resistivity. Fig. 3 observes the X-ray diffraction (XRD) spectrum for GZO thin film coating at different sputtering powers. Films are observed only at the (0 0 2) peak at $2\theta = 34.30^{o}$, showing the films are polycrystalline with a hexagonal wurtzite structure and a preferred orientation with the *c*-axis perpendicular to the substrates. The peak intensities become more intense and sharper with increasing R.F. power. Fig. 4 shows the SEM micrographs of GZO thin films deposited at R.F. power values of 50 W, 100 W and 200 W. The crystallite sizes increase upon increasing the sputtering power. These results are consistent with the XRD observation. Fig. 5 shows electrical resistivity of GZO thin films reduce with increased sputtering power.

Fig. 6 presents the SEM micrographs of GZO thin films coated at different substrate temperatures. The crystallite sizes enlarged with increased substrate temperature. Yamada et al. [25] show the improvement of the GZO film crystallinity with increasing substrate temperature up to 250 °C and obtained the lowest resistivity in GZO film at 250 °C. Fig. 7 shows as substrate temperature increased from room temperature to 100 °C, the electrical resistivities of the GZO thin films decreased from $8.33 \times 10^{-3}\ \Omega$ cm to $4.77 \times 10^{-3}\ \Omega$ cm. The high resistivity of the GZO thin films grown at lower

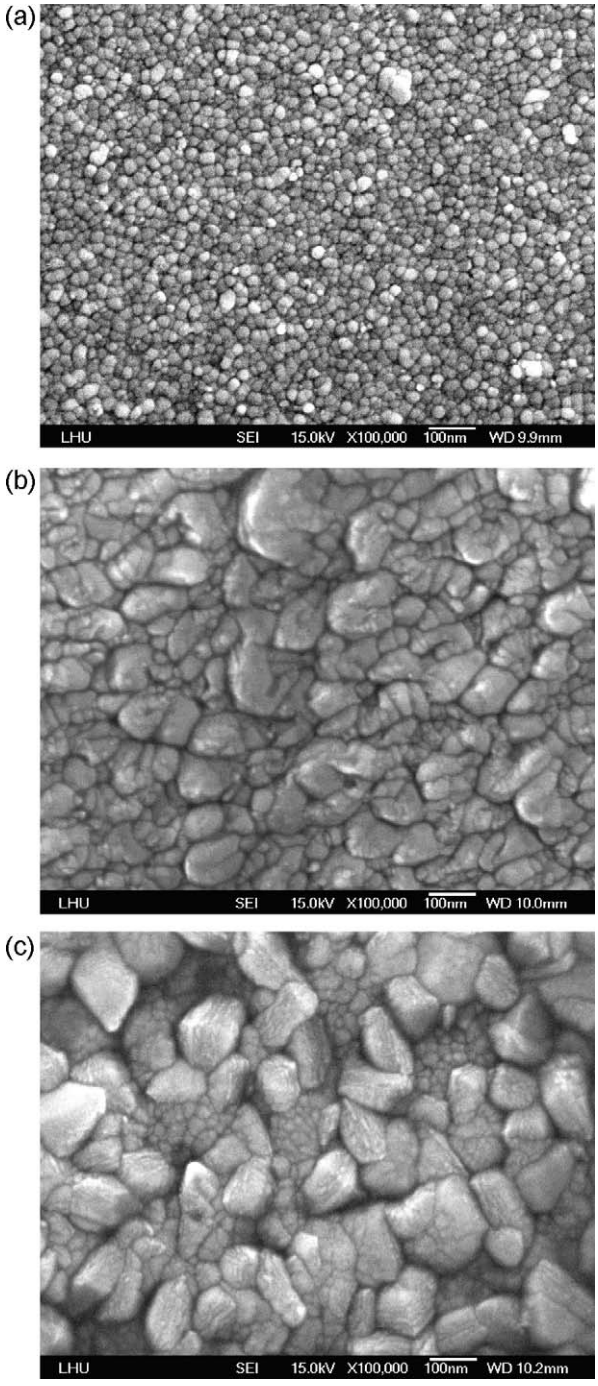

Fig. 4. SEM micrographs of as-deposited GZO thin films at R.F. power (a) 50 W, (b) 100 W and (c) 200 W tested after deposition for 60 min at substrate held at room temperature at sputtering pressure of 0.67 Pa.

temperatures is due to the low grain size and high values of surface roughness. At higher temperatures, the grains are comparatively larger and allow the carriers freely in the lattice leading a reduction in resistivity [26]. Therefore, the GZO thin films grown at substrate temperature of 100 °C showed a low electrical resistivity of $4.77 \times 10^{-3}\ \Omega$ cm. Fig. 8 shows the sputtering conditions (R.F. power: 200 W, sputtering pressure: 0.67 Pa, deposition time: 60 min and substrate temperature: room temperature) at different post-annealing treatments from

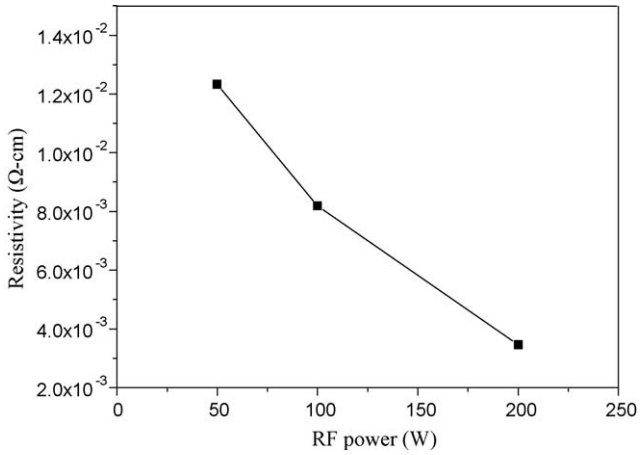

Fig. 5. Electrical resistivity of as-deposited GZO thin films at R.F. power tested after deposition for 60 min at substrate held at room temperature at sputtering pressure of 0.67 Pa.

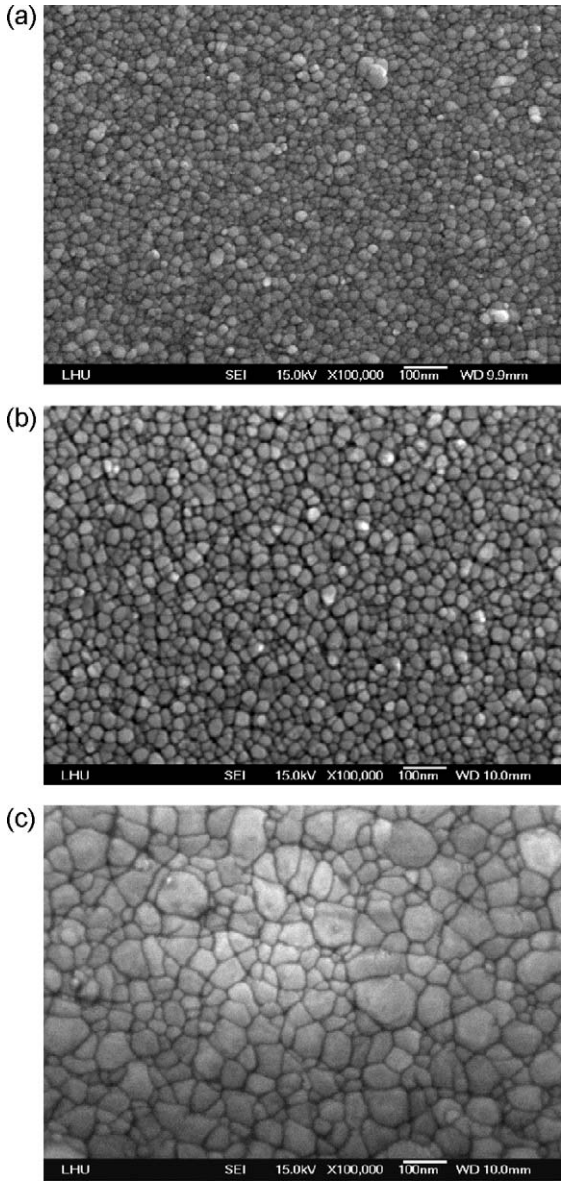

Fig. 6. SEM micrographs of as-deposited GZO thin films at different substrate temperatures (a) room temperature, (b) 50 °C and (c) 100 °C after deposition for 60 min at sputtering pressure and power of 0.67 Pa and 50 W, respectively.

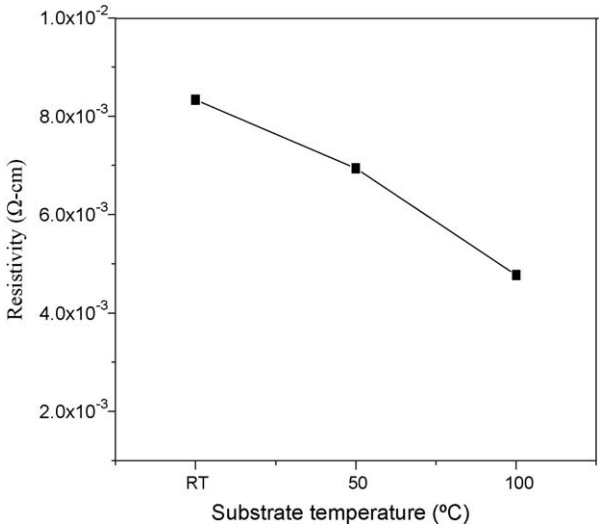

Fig. 7. Electrical resistivity of as-deposited GZO thin films after deposition for 60 min at different substrate temperatures at sputtering pressure and power of 0.67 Pa and 200 W, respectively.

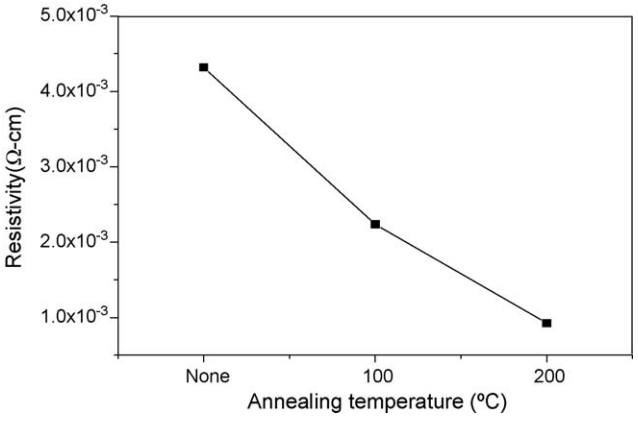

Fig. 8. Electrical resistivity of annealed GZO thin films deposited at room temperature for 60 min at sputtering pressure and power of 0.67 Pa and 200 W, respectively.

none to 200 °C. The results show that the electrical resistivity of GZO thin films decrease from $4.32 \times 10^{-3}\ \Omega\,\text{cm}$ to $9.235 \times 10^{-4}\ \Omega\,\text{cm}$. Major et al. [27] also found similar change in resistivity when annealed ZnO films in vacuum and oxygen.

Table 6 records the experimental results for transmittance and the corresponding S/N ratios. Table 7 lists the ANOVA results for transmittance. Note R.F. power ($P = 49.86\%$) and the deposition time ($P = 30.83\%$) are the most important variables affecting optical transmittance. The best combination to get higher optical transmittance is $A_1B_1C_1D_3E_3$. Fig. 9 shows the S/N response graph for transmittance. Experimental results reveal decreasing R.F. power and deposition time, but increasing substrate temperature and post-annealing temperature can obtain higher optical transmittance. However, these best combinations for the deposition rate, electrical resistivity and optical transmittance in sputtering parameters for Ga-doped ZnO film deposited on polymeric substrates are different.

Table 6
Experimental results for optical transmittance and S/N ratio.

Experimental no.	Control factors					Resistivity (10^{-3} Ω cm)		Mean value	Standard deviation	η (dB)
	A	*B*	*C*	*D*	*E*	1	2			
1	1	1	1	1	1	88.391	88.404	88.397	0.009	38.929
2	1	2	2	2	2	87.724	87.699	87.711	0.018	38.861
3	1	3	3	3	3	88.128	88.057	88.093	0.050	38.899
4	2	1	1	2	2	89.233	89.269	89.251	0.025	39.012
5	2	2	2	3	3	87.065	87.013	87.039	0.037	38.794
6	2	3	3	1	1	84.684	84.702	84.693	0.013	38.557
7	3	1	2	1	3	86.637	86.585	86.611	0.037	38.751
8	3	2	3	2	1	82.341	82.388	82.364	0.033	38.315
9	3	3	1	3	2	85.576	85.331	85.453	0.173	38.635
10	1	1	3	3	2	87.609	87.584	87.596	0.018	38.850
11	1	2	1	1	3	89.067	89.103	89.085	0.025	38.997
12	1	3	2	2	1	87.352	87.369	87.36	0.012	38.826
13	2	1	2	3	1	87.048	86.972	87.01	0.054	38.791
14	2	2	3	1	2	83.701	83.749	83.725	0.034	38.457
15	2	3	1	2	3	88.373	88.337	88.355	0.025	38.925
16	3	1	3	2	3	83.077	83.105	83.091	0.020	38.391
17	3	2	1	3	1	85.742	85.696	85.719	0.033	38.662
18	3	3	2	1	2	83.855	83.702	83.778	0.108	38.463

Table 7
ANOVA results for optical transmittance.

Factors	Level (dB)			DF	SS	*V*	*F*	$F_{0.05}$	*P* (%)
	1	2	3						
A	38.894	38.7561	38.536	2	0.390	0.195	24.353	4.46	49.86
B	38.788	38.681	38.717	2	0.035	0.018	2.200	4.46	4.50
C	38.860	38.748	38.578	2	0.241	0.121	15.057	4.46	30.83
D	38.692	38.722	38.772	2	0.019	0.010	1.211	4.46	2.48
E	38.680	38.713	38.793	2	0.040	0.020	2.518	4.46	5.16
Error				7	0.056	0.008			7.17
PE				(13)	(0.150)	(0.012)			(19.31)
Total				17	0.781				100

In order to acquire optimize sputtering parameters consideration to deposition rate, electrical resistivity and optical transmittance, an analysis of multiple performance characteristics is need. Based on Eqs. (7) and (8), the Grey relational grade and its ranking for each experiment using L_{18} orthogonal array is shown in Table 8. The higher Grey relational grade

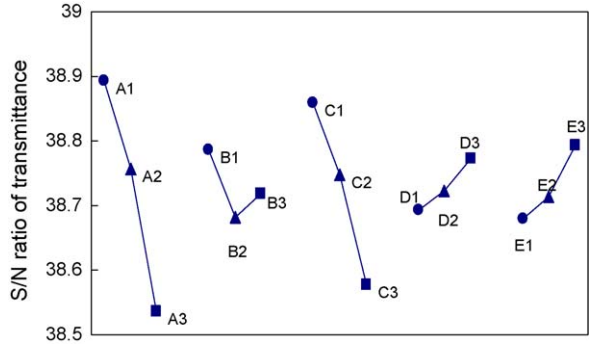

Fig. 9. S/N graph for transmittance.

Table 8
Grey relational grade and its order in the optimization process.

Experimental no.	Grey relational grade	Order
1	0.4894	16
2	0.4947	15
3	0.5313	12
4	0.6741	7
5	0.5760	10
6	0.4703	18
7	0.7699	2
8	0.7258	5
9	0.7593	3
10	0.5150	13
11	0.6115	9
12	0.4985	14
13	0.5356	11
14	0.4757	17
15	0.6130	8
16	0.7095	6
17	0.8247	1
18	0.7312	4

Table 9
Grey relational grade and its order for each deposition level.

Factor/level	Grey relational grade	Order
A1	0.5556	2
A2	0.4916	3
A3	0.7778	1
B1	0.5556	3
B2	0.7778	1
B3	0.5841	2
C1	0.7778	1
C2	0.5786	2
C3	0.5656	3
D1	0.3333	3
D2	0.4716	2
D3	1.0000	1
E1	0.5556	3
E2	0.5698	2
E3	0.7778	1

represents that the corresponding experimental result is closer to the ideal normalized value. In other words, the larger the Grey relational grade, the better will be the multiple performance characteristics. Since $(A_3B_2C_1D_3E_1)$ has the highest Grey relational grade as in experiment 17, it has the best multiple performance characteristics among all experiments. The mean value of the Grey relational grade for each coating parameter level is summarized in Table 9. The transmittance spectrum in the wavelength range of 400–800 nm for GZO thin films, using air as a reference, shows average transmittance at 82%. Fig. 10 point out the optical transmittance of GZO thin films improves with increased post-annealing temperature. However, the optical transmittance varies with a narrow range when the ZnO films were annealed at temperature lower than 500 °C [28].

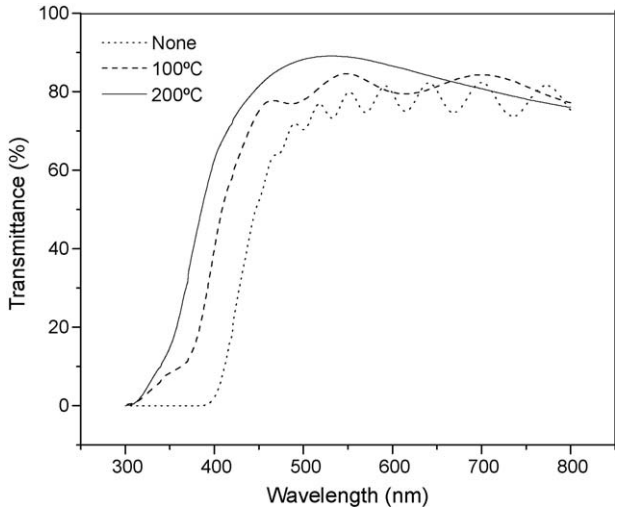

Fig. 10. Transmission spectra of annealed GZO thin films prepared using a sputtering power of 200 W (sputtering pressure of 0.67 Pa and deposition time 60 min for all samples).

Table 10
Results of confirmation test for multiple performance characteristics of GZO thin films.

Deposition rate	Electrical resistivity	Optical transmittance
Initial process parameters $A_3B_2C_1D_3E_1$		
21.033 nm/min	$1.194 \times 10^{-3}\ \Omega$ cm	86.148%
Grey theory prediction design $A_3B_2C_1D_3E_3$		
20.922 nm/min	$8.627 \times 10^{-4}\ \Omega$ cm	90%

6. Confirmation tests

Once the optimal design parameter level is selected, the final step predicts and verifies the quality characteristic improvement using the optimal design parameter level. Table 10 shows the coating experimental result for multiple performance characteristics of GZO thin films. A comparison of the Grey theory prediction design $(A_3B_2C_1D_3E_3)$ with the initial process parameters $(A_3B_2C_1D_3E_1)$ shows electrical resistivity decreases from $1.194 \times 10^{-3}\ \Omega$ cm to $8.627 \times 10^{-4}\ \Omega$ cm and optical transmittance increases from 86.148% to 90%, respectively. Figs. 11 and 12 show the optimal process

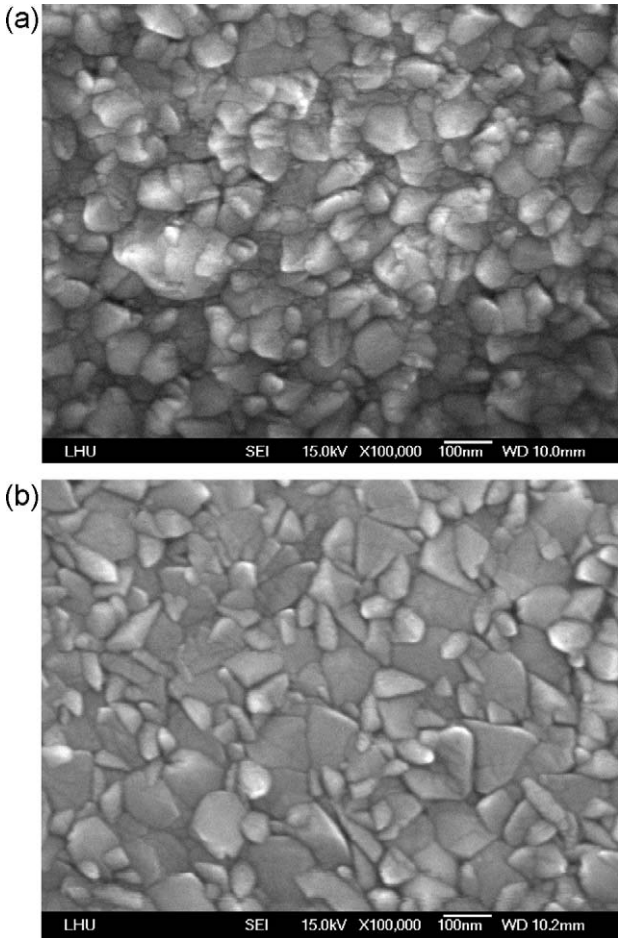

Fig. 11. SEM micrographs of GZO thin films obtained using deposition conditions chosen based on the initial process parameters and Grey theory prediction design: R.F. power, 200 W; sputtering pressure, 0.67 Pa; substrate temperature, 50 °C; deposition time, 30 min (a) without and (b) with post-annealing at 200 °C.

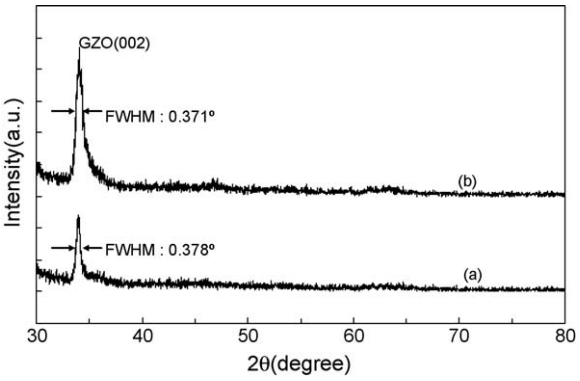

Fig. 12. X-ray diffraction patterns of GZO thin films obtained using deposition conditions chosen based on the initial process parameters and Grey theory prediction design: R.F. power, 200 W; sputtering pressure, 0.67 Pa; substrate temperature, 50 °C; deposition time, 30 min (a) without and (b) with post-annealing at 200 °C.

parameters in GZO thin films deposited on polyethylene terephthalate substrates. It can be seen from Fig. 11(b) that the surface morphology is improved with an increase in the post-annealing temperature. The minimum full-width at half-maximum (FWHM) for two XRD patterns without and with post-annealing as-deposited samples were 0.378° and 0.371°, respectively. According to the Scherrer formula, the mean grain sizes without and with post-annealing thin films were 21.96 nm and 22.38 nm, respectively [29]. However, the minimum FWHM for Grey theory prediction design ($A_3B_2C_1D_3E_3$) sample is smaller than initial process parameters ($A_3B_2C_1D_3E_1$) sample. These results are consistent with the SEM micrographs of GZO thin films shown in Fig. 11. So, the optimal process parameters in GZO thin films deposited on polyethylene terephthalate substrates can be effectively improved using the Grey–Taguchi method.

7. Conclusion

This paper presents the application of the Grey–Taguchi method to optimize GZO thin film deposition on the PET substrate with multiple performance characteristics. As a result, this method greatly simplifies the optimization of complicated multiple performance characteristics. The results are shown for the sputtering system with R.F. power: 200W, sputtering pressure: 0.67 Pa, deposition time: 30 min, substrate temperature: 100 °C and post-annealing temperature: 200 °C. The lowest electrical resistivity is $8.627 \times 10^{-4}\ \Omega$ cm and optical transmittance in the visible range is about 90%. The GZO thin films present better electrical and optical characteristics at a film thickness of roughly 600 nm (deposition rate 20.922 nm/min, deposition time 30 min).

Acknowledgement

The authors would like to thank the National Science Council of the Republic of China, Taiwan for financially supporting this research under Contract No. NSC 96-2622-E-262-008-CC3.

References

[1] H. Kim, J.S. Horwitz, G. Kushto, A. Pique, Z.H. Kafafi, C.M. Gilmore, D.B. Chrisey, Effect of film thickness on the properties of indium tin oxide thin films, Applied Physics 88 (10) (2000) 6021–6025.
[2] X. Yu, J. Ma, F. Ji, Y. Wang, C. Cheng, H. Ma, Thickness dependence of properties of ZnO:Ga films deposited by rf magnetron sputtering, Applied Surface Science 245 (2005) 310–315.
[3] M. Bender, E. Gagaoudakis, E. Douloufakis, E. Natsakou, N. Katsarakis, V. Cimalla, G. Kiriakidis, E. Fortunato, P. Nunes, A. Marques, R. Martins, Production and characterization of zinc oxide thin films for room temperature ozone sensing, Thin Solid Films 418 (1) (2002) 61–68.
[4] M.K. Jayaraj, K.J. Saji, K. Nomura, T. Kamiya, H. Hosono, Optical and electrical properties of amorphous zinc tin oxide thin films examined for thin film transistor application, Journal of Vacuum Science and Technology B: Microelectronics and Nanometer Structures 26 (2) (2008) 495–501.
[5] K. Ellmer, Resistivity of polycrystalline zinc oxide films: current status and physical limit, Journal of Physics D: Applied Physics 34 (21) (2001) 3097–3108.
[6] C.Y. Hsu, C.H. Tsang, Effects of ZnO buffer layer on the optoelectronic performances of GZO films, Solar Energy Materials & Solar Cells 92 (5) (2008) 530–536.
[7] J. Hu, R.G. Gordon, Atmospheric pressure chemical vapor deposition of gallium doped zinc oxide thin films from diethyl zinc, water, and triethyl gallium, Journal of Applied Physics 72 (11) (1992) 5381–5392.
[8] K.Y Cheong, N. Muti, S.R. Ramanan, Electrical and optical studies of ZnO:Ga thin films fabricated via the sol–gel technique, Thin Solid Films 410 (2002) 142–146.
[9] A.N. Banerjee, C.K. Ghosh, K.K. Chattopadhyay, H. Minoura, A.K. Sarkar, A. Akiba, A. Kamiya, T. Endo, Low-temperature deposition of ZnO thin films on PET and glass substrates by DC-sputtering technique, Thin Solid Films 496 (1) (2006) 112–116.
[10] T. Minami, H. Sato, H. Nanto, S. Takada, Group III impurity doped zinc oxide thin films prepared by RF magnetron sputtering, Journal of Applied Physics 24 (10) (1985) 781–784.
[11] P. Nunes, D. Costa, E. Fortunato, R. Martins, Performances presented by zinc oxide thin films deposited by r.f. magnetron sputtering, Vacuum 64 (2002) 293–297.
[12] S.S. Lin, J.L. Huang, D.F. Lii, The effect of thickness on the properties of Ti-doped ZnO films by simultaneous r.f. and d.c. magnetron sputtering, Surface Coating Technology 190 (2005) 372–377.
[13] V. Assuncao, E. Fortunato, A. Marques, H. Aguas, I. Ferreira, M.E.V. Costa, R. Martins, Influence of the deposition pressure on the properties of transparent and conductive ZnO:Ga thin-film produced by r.f. sputtering at room temperature, Thin Solid Films 427 (2003) 401–406.
[14] X. Yu, J. Ma, F. Ji, Y. Wang, X. Zhang, H. Ma, Influence of annealing on the properties of ZnO:Ga films prepared by radio frequency magnetron sputtering, Thin Solid Films 483 (2005) 296–300.
[15] E. Fortunato, A. Goncalves, V. Assuncao, A. Marques, H. Aguas, L. Pereira, I. Ferreira, R. Martins, Growth of ZnO:Ga thin films at room temperature on polymeric substrates: thickness dependence, Thin Solid Films 442 (2003) 121–126.
[16] Q.B. Ma, Z.Z. Ye, H.P. He, J.R. Wang, L.P. Zhu, B.H. Zhao, Substrate temperature dependence of the properties of Ga-doped ZnO films deposited by DC reactive magnetron sputtering, Vacuum 82 (2008) 9–14.
[17] G. Gonçalves, E. Elangovan, P. Barquinha, L. Pereira, R. Martins, E. Fortunato, Effect of rapid thermal annealing on electrical and optical properties of Ga doped ZnO thin films prepared at room temperature, Thin Solid Films 515 (24) (2007) 8562–8566.
[18] P.J. Ross, Taguchi Techniques for Quality Engineering, McGraw-Hill, New York, 1988.
[19] G. Taguchi, E.A. Elsayed, T. Hsaing, Quality Engineering in Production Systems, McGraw-Hill, New York, 1989.
[20] M.S. Phadke, Quality Engineering Using Robust Design, Prentice-Hall, Englewood Cliffs, NJ, 1989.
[21] J.L. Deng, Introduction to Grey system theory, The Journal of Grey System 1 (1) (1989) 1–24.

[22] Y.S. Tarng, S.C. Juang, C.H. Chang, J. Mater, The use of Grey-based Taguchi methods to determine submerged arc welding process parameters in hardfacing, Journal of Material Processing Technology 128 (2002) 1–6.
[23] K.T. Chiang, F.P. Chang, Optimization of the WEDM process of particle-reinforced material with multiple performance characteristics using Grey relational analysis, Journal of Material Processing Technology 180 (2006) 96–101.
[24] W.K. Chan, K.L. Tong, Multi-criteria material selections and end-of-life product strategy: Grey relational analysis approach, Material and Design 28 (2007) 1539–1546.
[25] T. Yamada, A. Miyake, S. Kishimoto, H. Makino, N. Yamamoto, T. Yamamoto, Effects of substrate temperature on crystallinity and electrical properties of Ga-doped ZnO films prepared on glass substrate by ion-plating method using DC arc discharge, Surface and Coatings Technology 202 (2007) 973–976.
[26] M. Devika, N. Koteeswara Reddy, K. Ramesh, V. Ganesan, E.S.R. Gopal, K.T. Ramakrishna Reddy, Influence of substrate temperature on surface structure and electrical resistivity of the evaporated tin sulphide films, Applied Surface Science 253 (3) (2006) 1673–1676.
[27] S. Major, A. Banerjee, K.L. Chopra, Annealing studies of undoped and indium-doped films of zinc oxide, Thin Solid Films 122 (1984) 31–43.
[28] R. Ghosh, G.K. Paul, D. Basak, Effect of thermal annealing treatment on structural, electrical and optical properties of transparent sol–gel ZnO thin films, Materials Research Bulletin 40 (11) (2005) 1905–1914.
[29] B.D Cullity, Elements of X-ray Diffraction, Addison-Wesley, Reading, MA, 1976.